Empirical Development of Radius of Bubble in Flow of Linear Elastic Fluids through a Converging-Diverging Nozzle

AHMED ZEESHAN^{1,2}, MUHAMMAD SHAHID NADEEM¹, NIKOS MASTORAKIS²

¹Department of Mathematics and Statistics, FOS, International Islamic University, H-10, Islamabad PAKISTAN

> ²Technical University of Sofia, BULGARIA

Abstract: - The basic aim of authors is develop an empirical relation for the radius of bubble versus the emerging parameters in modelling of the problem using sensitivity analysis procedure. The cavitating uni-dimensional bubbly flow of linear elastic fluid in a converging-diverging nozzle. The fields of mechanical engineering, shipping, environmental engineering, chemical engineering, and the medical sciences are just a few of the fields where bubbly flows are observed extensively. There are enormous applications of the bubble dynamics in engineering and medical. The geometry here considered is used in almost all mechanical machinery that includes automobiles, ships, pumps and valves etc. The cavitation tends to damage the wall of impact when bubble collapse or interact with neighbouring boundaries. The analysis helps to identify the behaviour of cavitating flow of bubbles subject to shape of nozzle and fluid properties. The equations of targeted flow are solved by RK-method using built-in function NDSolve in MATHEMATICA 10. The sensitivity analysis is performed using RSM (Response Surface Methodology) to identify the optimal response parameters affecting the flow. It is presented graphically that number of bubbles is an optimal parameter which is more sensitive as compared to other parameters involved. However elastic parameter and the cavitation number are also responsible to contribute in increase in sensitivity of radius and velocity and decrease in sensitivity of pressure.

Key-Words: - Cavitation, Rayleigh-Plesset equation, Kelvin-Voigt fluid, Linear Elastic Fluid, Nozzle flow, Sensitivity.

Received: April 9, 2025. Revised: August 3, 2025. Accepted: September 7, 2025. Published: November 17, 2025.

1. Introduction

Cavitation and bubble dynamics are fascinating phenomena that occur in fluid dynamics and have applications in various fields, including engineering, medicine, and environmental science. Cavitation refers to the formation and subsequent collapse of vapor-filled bubbles within a liquid when the local pressure drops below the vapor pressure of the liquid. This phenomenon can give rise to a wide array of intricate and substantial outcomes.

A major aspect of cavitation comprises its stimulus to the erosion and damage experienced by machinery and structures. The collapse of bubbles in vicinity of solid surfaces produces high-intensity shockwaves and micro jets, leading to erosion, pitting, and material wear. These dynamics are governed by principles derived from fluid mechanics, with a notable example being the Rayleigh-Plesset equation, which provides a mathematical description of how the radius of a spherical bubble changes over time [1]. In various medical procedures such as ultrasound imaging and lithotripsy, the deliberate use of controlled bubble cavitation serves therapeutic purposes, emphasizing the essential role played by bubble dynamics [2]. In the field of environmental science, cavitation and bubble dynamics are

ISSN: 2367-8992 14 Volume 9, 2025

particularly relevant in the setting of oceanography. The formation and collapse of bubbles in the ocean can produce subaquatic sounds referred to as "cavitation noise." These sounds offer a means to study and monitor oceanic processes, including the behavior of marine life [3].

It is crucial to comprehend that non-Newtonian qualities have much greater impact on cavitation or bubble dynamics than do Newtonian fluids, owing to its expanding use in variety of processes, including extrusion of polymers, lubrication with grease and heavy oils, coating of paper, use of plasma and mercury, nuclear fuel slurries, liquid alloys, food processing, biological processes, reactor cooling, heat exchangers, and few other applications. The topic of non-Newtonian fluid flow is growing in importance. These fluids include, but are not limited to, ice cream, paints, shampoos, mud, polymers and others. The well-known Navier-Stokes equation cannot pretend fluid flow that is not Newtonian. It is quite challenging to solve nonlinear constitutive equations representing viscous flows. Viscous fluids fall into one of these three categories: integral, differential, or rate type fluids. Viscoelastic fluid is subclass of fluid of rate type. The largest increase in viscosity of polymer solutions in an extensional flow, such as that created around a spherical bubble during its expansion or collapse phase, is the most notable outcome. Polymers are forced apart in absence of applied flow field, and their length can increase by three orders of magnitude in direction of extension. Because of this, solution is able to sustain far greater stresses, and squeezing is lessened where polymers are stretched. Additionally, a lot of biological fluids, such as saliva, synovial fluid and blood, exhibit viscoelasticity and non-Newtonian properties [4]. The importance of cavitation in the advancement of current ultrasonic and laser-assisted surgical methods makes this a vital topic. The scientific literature lacks thorough description of the fundamental mechanisms underlying cavitation in non-Newtonian its expanding fluids. despite bioengineering applications. Given the diversity of the components necessary for understanding the associated processes, this is not surprising.

In the literature, several constitutive equations are used to characterize the behavior of non-Newtonian fluids. The Maxwell and Oldroyd-B models have greatly exceeded expectations and anticipation. Their relative simplicity has undoubtedly been appealing, particularly in the case

of numerical simulation of viscoelastic flows, where simple models have been critical in developing numerical techniques. Dumbbell and the KBKZ model are two more prominent viscoelastic models that had widely employed. Shima et al. [5] conducted a study to examine the behavior of an individual spherical bubble immersed in a sound field within a purely viscous liquid, Tsujino et al. [6], and Brujan [7]. Also, Shima et al. [8] investigated bubble oscillations by employing a linear viscoelastic model to characterize the rheological properties of the liquid. Ting [9] employed an Oldroyd three-constant model that incorporates characteristic relaxation and retardation times, which are used to scale the covariant convected time derivatives of stress and strain rate. Additionally, he considered thermal effects arising from the phase changes of water, such as evaporation or condensation. The resulting integro-differential equation was solved numerically for a solution containing 500 ppm of polyethylene (PEO). Ting's conclusion was viscoelasticity has a minimal retardation effect on bubble growth and collapse, provided that the material constants align with the properties of dilute polymer solutions. Furthermore, Ting's work suggests that heat and mass transfer effects are not significant under cavitation conditions. In a separate study, a rigorous experimental study was conducted and a numerical exploration was made of a Venturi reactor characterized by a pronounced choking effect. This investigation employed a custom-developed, state-of-the-art compressible cavitation phase-change solver to gain insights into the flow dynamics and underlying choking mechanisms in cavitationinduced choked flow scenarios [10].

Zana and Leal [10] numerically tackled the conservation equations for mass and momentum, as well as a gas diffusion equation, to analyze the collapse of a single bubble. The impact of viscoelastic medium or fluid on the oscillations of bubbles, is due to Fogler and Goddard [11]. One of the most intriguing findings was that the presence of elasticity can delay bubble collapse and cause prolonged oscillatory motion. A recent contribution to studies involving cavitation is viscoelastic materials using different constitutive equations of non-Newtonian fluids has been discussed by Fogler and Goddard [11], Shima and Tsujino [12], Allen and Roy [13-14], Gaudron et al. [15]. Since the viscoelastic materials behave like tissues so to discuss the cavitation in the tissues of living

organism it is felt appropriate to discuss cavitation in viscoelastic materials. Initially to study tissues most of the researcher has considered Maxwell-type fluid models. However based on the property of relaxation to its original structure in tissues studies suggested that it will be far more better to use Kelvin-Voigt models instead of using Maxwell-type models [15].

Tangren et al. [16] has presented his study of bubbly flow through nozzles and ducts. Later on discussion on these type of flows was made by Wang and Brennen [17]. A comprehensive investigation into the essential flow characteristics of vortex-based cavitation devices, employing both experimental and computational approaches was performed [18], the study encompassed a wide spectrum, encompassing the simulation of cavitating flows within these devices across a diverse range of viscosity levels and device scales. For experimental endeavors, the aqueous glycerol solutions with viscosities spanning up to 800 centipoise (cP) was taken. It is effectively identified the inception of cavitation through the analysis of acoustic signals, providing valuable insights into the behavior of cavitating flows in these systems. Effects of non-dimensional parameters on such flows in Newtonian fluid were depicted by Zamoum & Kessel [19] while in presence of elastic/viscoelastic fluids (neo-Hookean, elastic and Mooney Rivlin) in nozzles and channels were presented by Zeeshan et al. [20-21]. Effect of surface materials on the surface of hydrofoils are investigated by Hao et al. [22].

A one-dimensional bubbly mixing of fluid in ducts and nozzles is one of straightforward flow combinations of liquid and gas. In many applications in engineering and the medical sciences, it is a significant problem. A low-pressure area causes the flow past a nozzle to cavitate, which causes the flow to quicken. A barotropic relation, $p = f(\rho)$, can be constructed in some bubbly flows if the fluid pressure is expected to be only a function of fluid density. All effects caused by bubble contents—aside from compressibility—are insignificant, and the bubbly mixture can be thought of as a single-phase compressible flow.

Motivated by all above contributions, the authors have considered the cavitating flow of Kelvin-Voigt (linear elastic) fluid through a converging-diverging nozzle. The schematic of the flow is shown in **Figure 1**. Utilizing built-in functions, the RK technique is used along with the symbolic computation

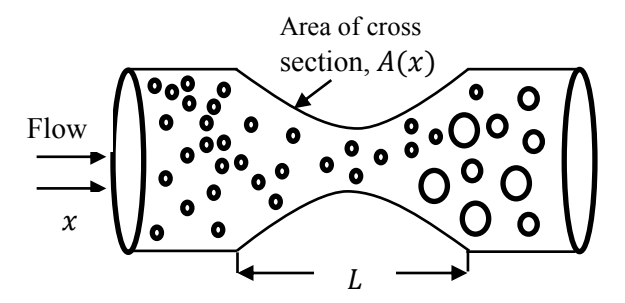
programme MATHEMATICA and the package NDSolve to identify singularity or state changes in a problem and then take appropriate action, such as restarting the integration. Effectively acting as a controller method, the NDSolve "EventLocator" method searches for measures and takes the necessary action, while integration of differential system is otherwise fully left to an underlying methodology [23]. By setting elasticity parameter to zero, the Newtonian formulation of Zamoum & Kessel may be retrieved for the validity of the results. The steady state solutions revealed two distinct flow regimes, referred to as quasi-steady and quasiunsteady [19–21]. The former is distinguished by the significant spatial fluctuations caused by the cavitation bubbles' pulsations downstream of the throat. To flashing flow, the quasi-unsteady solutions relate. As the flow moves from one area to another, bifurcation happens [19–21]. We displayed the flow characteristics under the influence of various factors while purposefully limiting ourselves to the zone known as stable region, where neither flashing nor bifurcation happens. Furthermore, related studies can be found in [24-32] to have insight of the flows in non-Newtonian and especially viscoelastic materials

Equations of the said flow were initially solved to find the data points, usually termed as outcomes of an experiment. Response Surface Methodology (RSM)[33] is used to analyze the potentially significant input parameter(s) from the list of involved parameters. RSM is a statistical and mathematical technique used to predict the behavior of an underlying system on the basis of experimental data. Here the experimental data or set of points are the computational values of the output responses obtained by numerically solving the system of equations due to varying input responses. A statistical experimental design is developed by using the central composite design. Three input parameters, the cavitation number, the modulus of elasticity or elastic parameter and number of bubbles are taken into account whose impacts on the output parameters, the radius of the bubble, the velocity of flow and minimum pressure coefficient is sought. Correlations are developed using RSM between input and output responses of the flow problem. We have never before studied the sensitivity analysis of cavitating flow of linear elastic fluid in a converging-diverging nozzle. We have now covered how the Reynolds number, Weber number, void percent, and elastic modulus

affect the flow's radius, pressure coefficient, and velocity. Other studies related to sensitivity analysis

2 Problem Formulation

In the current article, flow of contaminant, air bubbles are considered through various geometries in



elastic fluid (Second-Grade Fluid). Continuum mechanics formalism is used to describe the dynamics of bubbles.

Fig.1: Cavitating flow of bubbly mixture through a nozzle (converging-diverging)

The nozzle described in above figure, mathematically is described in (1).

$$A(x) = \begin{cases} \left\{ 1 - \frac{1}{2} C_{PMIN} \left[1 - \cos\left(\frac{2\pi x}{L}\right) \right] \right\}^{-\frac{1}{2}}; 0 \le x \le L \\ 1; \quad 0 < x \text{ and } x > L \end{cases}$$
 (1)

Equations of continuity and momentum for bubbly flow are given as [16]

$$\frac{\partial}{\partial t} \left[\left(-\alpha + 1 \right) A \right] + \frac{\partial}{\partial x} \left[\left(-\alpha + 1 \right) u A \right] = 0 \tag{2}$$

$$u\frac{\partial u}{\partial x} + \frac{\partial u}{\partial t} = -\frac{1}{2(1-\alpha)}\frac{\partial C_p}{\partial x}$$
 (3)

here, $\alpha(x,t)$ denotes the void fraction, it depends on R(x,t) as stated below

$$\alpha(x,t) = \frac{4\pi\eta R^3}{3 + 4\pi\eta R^3} \tag{4}$$

 C_{p} , denotes the fluid pressure coefficient stated as

of flow behavior could be found in [34-35].

$$C_p = \frac{2(P_{\infty}(t) - P_{\infty})}{\rho_l u_s^2} \tag{5}$$

and η is the population of bubble per unit of volume. The RP equation for a bubbly mixture of a non-Newtonian fluid is described in (8), where we have considered in our study a second-grade fluid for which last, the integral term on the right hand side is separately evaluated.

$$R\frac{D^{2}R}{Dt^{2}} + \frac{3}{2} \left(\frac{DR}{Dt}\right)^{2}$$

$$= \frac{1}{\rho_{l}} \left\{ \left(P_{B} - P_{\infty}(t)\right) - \frac{2S}{R} - P_{ext} + 3\int_{R}^{\infty} \frac{\tau_{rr}}{r} dr \right\}$$
(6)

D/Dt the Lagrangian derivative, is defined in (7), R, v_l, ρ_l, S, P_B and $P_{\infty}(t)$ are radius, viscosity, density, surface tension, pressure inside the bubble and pressure far away from the bubble wall respectively.

$$\frac{D}{Dt} = \frac{\partial}{\partial t} + u \frac{\partial}{\partial x} \tag{7}$$

Presence of some contaminant gas made us to choose its partial pressure termed here as P_G and some water vapour (or the vapour of considered fluid) P_{ν} . On the assumption that the gas entrapped, is incondensable the partial pressure is described as [21].

$$P_G = P_{G_0} \left(\frac{R_0}{R}\right)^{3k} \tag{8}$$

where P_{G_0} is the initial partial pressure in interior of the bubble, k and R_0 , being poly-tropic index and initial radius of the bubble, subsequently, the total pressure inside the bubble and initial partial pressure are described below.

$$P_{B} = P_{G} + P_{v} = P_{v} + (R_{0} / R)^{3k} P_{G_{0}}$$
(9)

$$P_{G_0} = P_{\infty} - P_{\nu} + (2S / R_0) \tag{10}$$

ISSN: 2367-8992 17 Volume 9, 2025

Let P_{ext} is the pressure field that is applied externally to the bubble and P_{si} is linked to the pressure that other bubbles diffuse and the pressure that any other exterior field applies to the bubble i. The poly-tropic index, the value for gas is provided in the literature as 1.4, is used to calculate this relationship.

$$P_{ext} = P_{si} + P_{A,i}(t) \tag{10a}$$

where pressure disseminated by other bubbles defined in (14) as

$$P_{si} = \sum_{j \neq 1}^{n_B} \frac{\rho_l}{d_{ij}} \frac{D}{Dt} \left(R_j^2 \frac{DR_j}{Dt} \right)$$
(11)

where $d_{ij} = d_{ji}$ is distance of bubble i from bubble j and vice versa. Using Eqn. (13) and (14) in Eqn. (8) produces

$$R\frac{D^{2}R}{Dt^{2}} + \frac{3}{2} \left(\frac{DR}{Dt}\right)^{2} = \frac{P_{B} - P_{\infty}(t)}{\rho_{l}} - \frac{2S}{\rho_{l}R} - \frac{1}{\rho_{l}}$$

$$\times \left(\sum_{j\neq 1}^{n_{B}} \frac{\rho_{l}}{d_{ij}} \frac{D}{Dt} \left(R_{j}^{2} \frac{DR_{j}}{Dt}\right) + P_{A,i}(t)\right) + \frac{3}{\rho_{l}} \int_{R}^{\infty} \frac{\tau_{rr}}{r} dr$$
 (12)

The distance $D = d_{ij} = d_{ji}$ between each bubble and the others is assumed to be constant, and it is also assumed that all of the bubbles are subject to the same external pressure field $P_{A,i}(t) = P(t)$, which here is considered to be negligibly small due to which Eqn. (13) takes the form shown in Eqn. (16) for which the initial conditions are stated in eqn. (17).

$$R\frac{D^2R}{Dt^2} + \frac{3}{2} \left(\frac{DR}{Dt}\right)^2 = \frac{P_B - P_\infty(t)}{\rho_l} - \frac{2S}{\rho_l R}$$
$$-\frac{(n-1)}{D} \left(R^2 \frac{D^2R}{Dt^2} + 2R \left(\frac{DR}{Dt}\right)^2\right) + \frac{3}{\rho_l} \int_{R}^{\infty} \frac{\tau_{rr}}{r} dr \quad (13)$$

$$R_s = R, 0 = \frac{dR}{dx}, u_s = u, P_s = P \text{ at } x = 0$$
 (14)

For steady-state solutions equations (2-3) becomes

$$uA(1-\alpha) = (1-\alpha_s) = \text{constant}$$
 (15)

$$\frac{dC_p}{dx} = -2(1-\alpha)u\frac{du}{dx} \tag{16}$$

Eqn. (29) is obtained by using non-dimensional variables described in (28) in eqn. (16)

$$\overline{A} = \frac{A}{A_{s}}, \overline{L} = \frac{L}{R_{s}}, \overline{R} = \frac{R}{R_{s}}, \overline{A} = \frac{A}{A_{s}}, \overline{u} = \frac{u}{u_{s}},
\overline{x} = \frac{x}{R_{s}}, \overline{t} = \frac{tu_{s}}{R_{s}}, \overline{\rho} = \frac{\rho_{l}}{\rho_{s}}, \overline{\eta} = \eta R_{s}^{3}
R \frac{D^{2}R}{Dt^{2}} + \frac{3}{2} \left(\frac{DR}{Dt}\right)^{2} = A - \frac{\sigma}{2} \left(1 - \frac{1}{R^{3k}}\right)
- \frac{2}{We} \left(\frac{1}{R} - \frac{1}{R^{3k}}\right) - \frac{(n-1)R_{s}u_{s}^{2}}{D}
\times \left(R^{2} \frac{D^{2}R}{Dt^{2}} + 2R \left(\frac{DR}{Dt}\right)^{2}\right) - \frac{C_{p}}{2} - P_{A}$$
(18)

Where use of the Lagrangian derivative deliberated earlier, reduces above eqn. (17) and (13) as given below,

$$R\left(u^{2} \frac{d^{2}R}{dx^{2}} + u \frac{du}{dx} \frac{dR}{dx}\right) \left(1 - \frac{n-1}{d} R_{s} u_{s}^{2} R\right)$$

$$+ \frac{3u^{2}}{2} \left(\frac{dR}{dx}\right)^{2} + 2\left(\frac{n-1}{d}\right) R_{s} u_{s}^{2} R \left(\frac{dR}{dx}\right)^{2}$$

$$+ \frac{\sigma}{2} \left(1 - \frac{1}{R^{3k}}\right) + \frac{2}{We} \left(\frac{1}{R} - \frac{1}{R^{3k}}\right) + \frac{C_{p}}{2}$$

$$+ f(R, u, x) = 0$$

$$R = 1, \frac{dR}{du} = 0, u = 0 \text{ and } C_{p} = 0 \text{ at}$$
(19)

where, is the Weber number $We = \rho_l R_s u_s^2 / S$, f(R,u,x) is non-dimensional form of r.h.s of eqn. (26) which is given in (33) and $\sigma = 2(P_x - P_y) / \rho_l u_s^2$ is the cavitation number

(20)

$$f(R,u,x) = -\frac{4u}{\operatorname{Re}R} \frac{dR}{dx} - 2\gamma \left(1 - \frac{1}{R^2}\right) \tag{21}$$

x = 0

Coupled Eqs. (15-16) & Eqs. (19-21) are solved by RK –Method to find the unknown variables involved, which in detail is discussed in the following section.

3 Sensitivity Analysis

The impacts of three input parameters, the elasticity parameter n (number of bubbles), Reynolds number (Re) and elasticity parameter (γ) on the three output responses the radius, velocity and the pressure coefficient are examined in this chapter. The optimal parameter is obtained using Response Surface Methodology (RSM) by carrying out the sensitivity analysis of the effective parameters on the flow of a cavitating uni-dimensional, linear elastic fluid through a converging-diverging nozzle. The ranges taken in this study of the input parameter whose responses are to be determined towards output responses are as follows:

- a. Number of bubbles (n) varied from 2 to 4.
- b. Reynolds number (Re) varied from 200 to 500.
- c. Elasticity parameter (γ) varied from 0.001 to 0.1.

The value of x has been set at x = 8, inside of the converging-diverging section of the nozzle to obtain the numerical data used in the analysis and presented in the Table 2.To perform sensitivity analysis 20 runs of an experiment are considered. Table 1 defines the ranges of parameters (input) while on solving the corresponding differential equations of the flow, the values of output responses, the radius, the velocity and the pressure are listed in **Table 2**. Results of the variance analysis (ANOVA) for dependent variables, the radius, the velocity and the pressure are furnished in **Tables 3-5**. Here important aspects in these tables are the F-values and P-values in ANOVA analysis. The F-value are representatives of the variation in the data while P-values are the representatives of the probability validation of the model's accuracy. Larger F-values are directives for the significance of the results while in case of P-

values, lower values supports the significance. Consequently, both values considered together to have strong agreement for the significance of the results. Table 6 demonstrates the estimated regression coefficients on the basis of discussed criteria. From where we see that in case of the three dependent variables radius, velocity and pressure in terms of the coded parameters significant terms are constant, A, C, A^2 and AC while other terms B, C, B^2, C^2, AB and BC become insignificant on the basis of higher P-values and lower F-values. Also their contribution to the results is given in **Table 3-5**. seems to be too small to be considered. Residual errors generally are attributed to the un-matched data points to the regression line whereas lack-of-Fit exhibits when model is unable to describe the connectedness between the input and output parameters. The graphs of residuals for radius, velocity and pressure are elaborated in Figures 2(ac)-4(a-c) respectively which shows that errors are normally distributed along the straight line and hence are well-fitted

Equations for radius, velocity and pressure are given in eqns. (22-24). Sensitivity of the radius, velocity and pressure are their partial derivatives, given in eqns. (25-33). Values of sensitivity for radius, velocity and pressure are obtained by taking A = 0, the lower value, and by varying the values of B and C. **Table 7** (a-c) demonstrates the values obtained for sensitivity of the three output variables while graphs for these values are presented in **Figures 5**(a-c)-7 (a-c).

Table 1: Input variables and their domains used in the statistical analysis

| Variable | Symbol | -1 | 0 | +1 |
|-----------|--------|-------|--------|-----|
| Number of | n | 2 | 3 | 4 |
| Bubbles | | | | |
| Reynolds | Re | 200 | 350 | 500 |
| number | | | | |
| Elastic | γ | 0.001 | 0.0505 | 0.1 |
| parameter | | | | |

ISSN: 2367-8992 19 Volume 9, 2025

Table 2: The computed values for this experiment against the randomly designated values of input response

| Run | Coo | lal Va | lues | Input Responses | | | | Output Response | es |
|-------|-----|--------|------|-----------------|-----|--------|------------|-----------------|--------------|
| Order | A | В | С | n | Re | γ | R (radius) | u (velocity) | P (pressure) |
| 1 | 0 | 0 | 0 | 3 | 350 | 0.0505 | 1.09049 | 1.16116 | -0.347475 |
| 2 | 0 | -1 | 0 | 3 | 200 | 0.0505 | 1.09047 | 1.16116 | -0.347474 |
| 3 | 1 | 0 | 0 | 4 | 350 | 0.0505 | 1.06389 | 1.16078 | -0.346478 |
| 4 | 1 | 1 | 1 | 4 | 500 | 0.1000 | 1.06355 | 1.16078 | -0.346466 |
| 5 | 1 | -1 | 1 | 4 | 200 | 0.1000 | 1.06353 | 1.16078 | -0.346466 |
| 6 | -1 | -1 | -1 | 2 | 200 | 0.0010 | 1.15833 | 1.16220 | -0.350249 |
| 7 | 0 | 0 | 0 | 3 | 350 | 0.0505 | 1.09049 | 1.16116 | -0.347475 |
| 8 | -1 | 0 | 0 | 2 | 350 | 0.0505 | 1.15630 | 1.16217 | -0.350163 |
| 9 | 0 | 0 | -1 | 3 | 350 | 0.0010 | 1.09119 | 1.16117 | -0.347501 |
| 10 | 0 | 0 | 0 | 3 | 350 | 0.0505 | 1.09049 | 1.16116 | -0.347475 |
| 11 | 0 | 0 | 0 | 3 | 350 | 0.0505 | 1.09049 | 1.16116 | -0.347475 |
| 12 | 0 | 0 | 0 | 3 | 350 | 0.0505 | 1.09049 | 1.16116 | -0.347475 |
| 13 | 0 | 0 | 0 | 3 | 350 | 0.0505 | 1.09049 | 1.16116 | -0.347475 |
| 14 | 0 | 1 | 0 | 3 | 500 | 0.0505 | 1.09050 | 1.16116 | -0.347476 |
| 15 | -1 | -1 | 1 | 2 | 200 | 0.1000 | 1.15413 | 1.16213 | -0.350072 |
| 16 | -1 | 1 | -1 | 2 | 500 | 0.0010 | 1.15844 | 1.16220 | -0.350253 |
| 17 | 1 | -1 | -1 | 4 | 200 | 0.0010 | 1.06422 | 1.16079 | -0.346490 |
| 18 | 1 | 1 | -1 | 4 | 500 | 0.0010 | 1.06424 | 1.16079 | -0.346491 |
| 19 | 0 | 0 | 1 | 3 | 350 | 0.1000 | 1.08980 | 1.16115 | -0.347449 |
| 20 | -1 | 1 | 1 | 2 | 500 | 0.1000 | 1.15423 | 1.16214 | -0.350076 |

 Table 3: Results of variance analysis of radius of the bubble

| Source | DF | Adj SS | Adj MS | F-Value | P-Value |
|-------------------|----|----------|----------|-----------|---------|
| Model | 9 | 0.023283 | 0.002587 | 57761.88 | 0.000 |
| Linear | 3 | 0.021357 | 0.007119 | 158949.83 | 0.000 |
| N | 1 | 0.021344 | 0.021344 | 476570.23 | 0.000 |
| Re | 1 | 0.000000 | 0.000000 | 0.18 | 0.685 |
| Gamma | 1 | 0.000012 | 0.000012 | 279.08 | 0.000 |
| Square | 3 | 0.001920 | 0.000640 | 14289.82 | 0.000 |
| n*n | 1 | 0.001057 | 0.001057 | 23590.01 | 0.000 |
| Re*Re | 1 | 0.000000 | 0.000000 | 0.01 | 0.945 |
| gamma*gamma | 1 | 0.000000 | 0.000000 | 0.00 | 0.994 |
| 2-Way Interaction | 3 | 0.000006 | 0.000002 | 46.00 | 0.000 |
| n*Re | 1 | 0.000000 | 0.000000 | 0.08 | 0.782 |
| n*gamma | 1 | 0.000006 | 0.000006 | 137.93 | 0.000 |
| Re*gamma | 1 | 0.000000 | 0.000000 | 0.00 | 0.987 |
| Error | 10 | 0.000000 | 0.000000 | | |
| Lack-of-Fit | 5 | 0.000000 | 0.000000 | | |
| Pure Error | 5 | 0.000000 | 0.000000 | | |
| Total | 19 | 0.023284 | | | |

ISSN: 2367-8992 20 Volume 9, 2025

Table 4: Results of variance analysis of velocity of the bubble

| Source | DF | Adj SS | Adj MS | F-Value | P-Value |
|-------------------|----|----------|----------|-----------|---------|
| Model | 9 | 0.000005 | 0.000001 | 36596.54 | 0.000 |
| Linear | 3 | 0.000005 | 0.000002 | 99400.17 | 0.000 |
| N | 1 | 0.000005 | 0.000005 | 298020.03 | 0.000 |
| Re | 1 | 0.000000 | 0.000000 | 0.62 | 0.448 |
| Gamma | 1 | 0.000000 | 0.000000 | 179.86 | 0.000 |
| Square | 3 | 0.000000 | 0.000000 | 10357.57 | 0.000 |
| n*n | 1 | 0.000000 | 0.000000 | 17030.98 | 0.000 |
| Re*Re | 1 | 0.000000 | 0.000000 | 0.04 | 0.855 |
| gamma*gamma | 1 | 0.000000 | 0.000000 | 0.04 | 0.855 |
| 2-Way Interaction | 3 | 0.000000 | 0.000000 | 31.90 | 0.000 |
| n*Re | 1 | 0.000000 | 0.000000 | 0.78 | 0.398 |
| n*gamma | 1 | 0.000000 | 0.000000 | 94.13 | 0.000 |
| Re*gamma | 1 | 0.000000 | 0.000000 | 0.78 | 0.398 |
| Error | 10 | 0.000000 | 0.000000 | | |
| Lack-of-Fit | 5 | 0.000000 | 0.000000 | | |
| Pure Error | 5 | 0.000000 | 0.000000 | | |
| Total | 19 | 0.000005 | | | |

Table 5: Results of variance analysis of pressure

| Source | DF | Adj SS | Adj MS | F-Value | P-Value |
|-------------------|----|----------|----------|-----------|---------|
| Model | 9 | 0.000038 | 0.000004 | 43863.29 | 0.000 |
| Linear | 3 | 0.000034 | 0.000011 | 119023.76 | 0.000 |
| N | 1 | 0.000034 | 0.000034 | 356853.47 | 0.000 |
| Re | 1 | 0.000000 | 0.000000 | 0.13 | 0.729 |
| Gamma | 1 | 0.000000 | 0.000000 | 217.69 | 0.000 |
| Square | 3 | 0.000004 | 0.000001 | 12525.34 | 0.000 |
| n*n | 1 | 0.000002 | 0.000002 | 20669.48 | 0.000 |
| Re*Re | 1 | 0.000000 | 0.000000 | 0.00 | 0.994 |
| gamma*gamma | 1 | 0.000000 | 0.000000 | 0.00 | 0.994 |
| 2-Way Interaction | 3 | 0.000000 | 0.000000 | 40.78 | 0.000 |
| n*Re | 1 | 0.000000 | 0.000000 | 0.06 | 0.805 |
| n*gamma | 1 | 0.000000 | 0.000000 | 122.27 | 0.000 |
| Re*gamma | 1 | 0.000000 | 0.000000 | 0.00 | 0.972 |
| Error | 10 | 0.000000 | 0.000000 | | |
| Lack-of-Fit | 5 | 0.000000 | 0.000000 | * | * |
| Pure Error | 5 | 0.000000 | 0.000000 | | |
| Total | 19 | 0.000038 | | | |

ISSN: 2367-8992 21 Volume 9, 2025

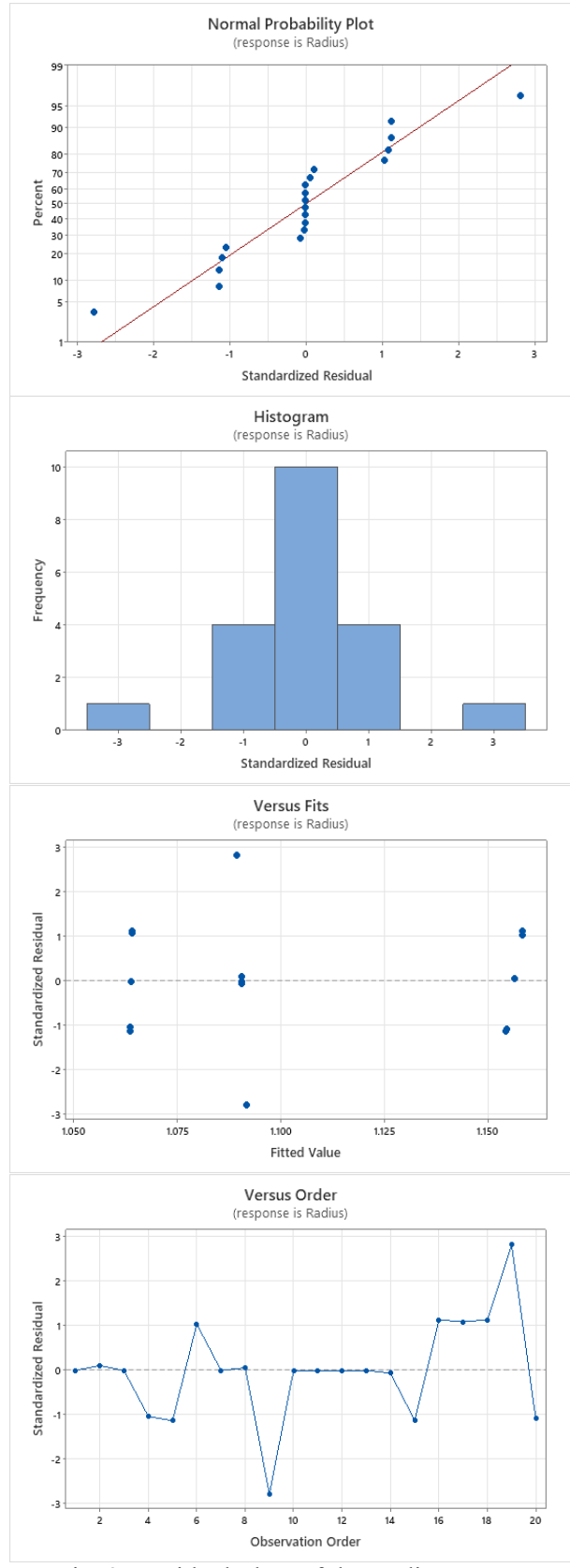


Fig. 2: Residual Plots of the Radius

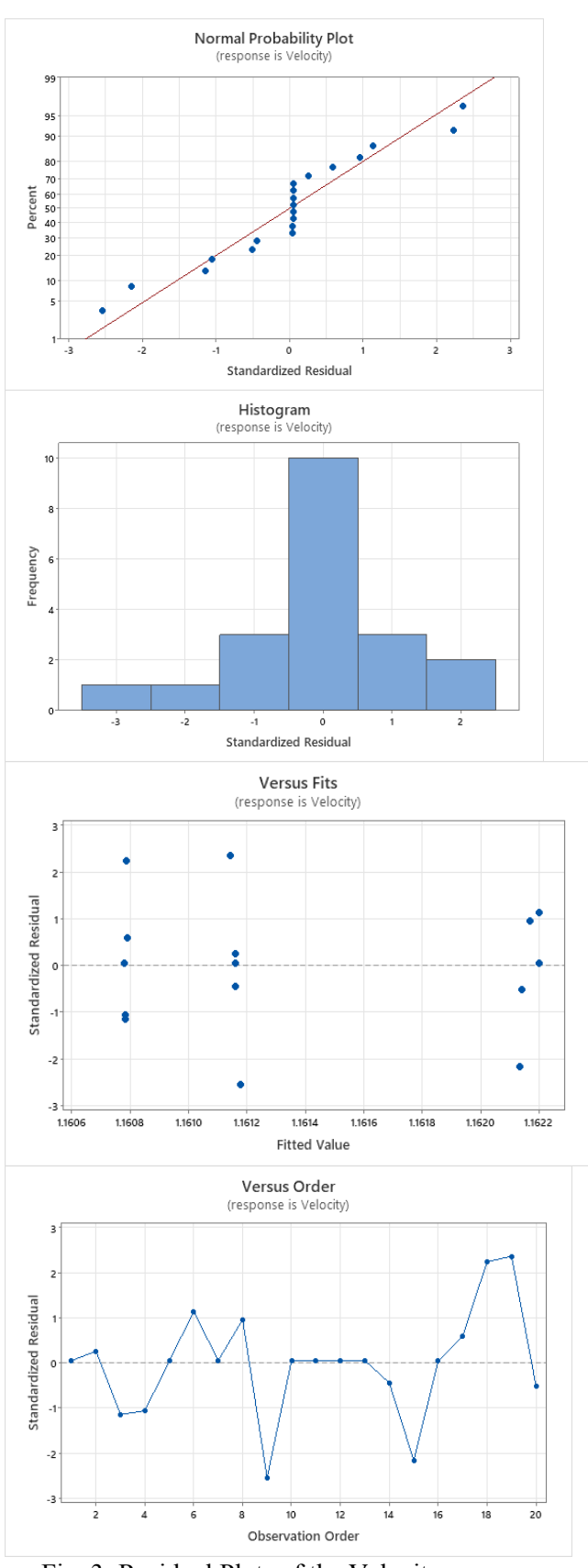


Fig. 3: Residual Plots of the Velocity

ISSN: 2367-8992 22 Volume 9, 2025

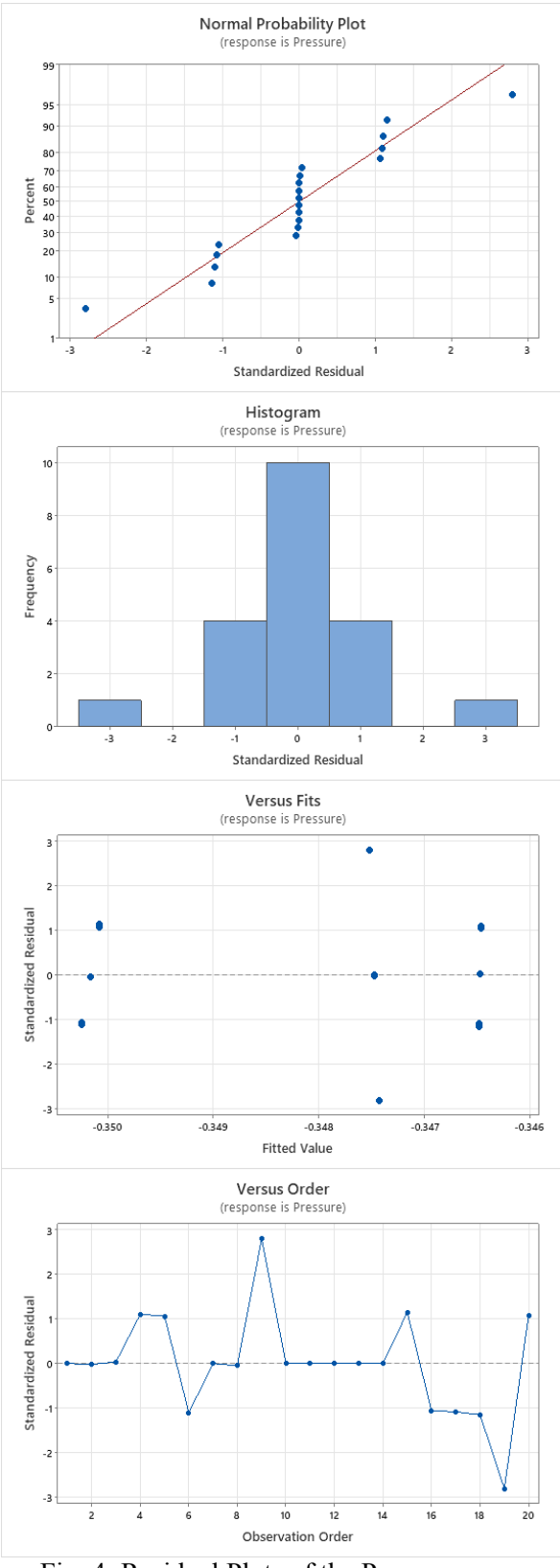


Fig. 4: Residual Plots of the Pressure

Table 6
Estimated regression coefficients for radius, velocity and pressure

| and pressure | | |
|-----------------------------|---------------|------------------|
| Term | Coefficient | P-value |
| Radius | 1 000 10 | 0.000 |
| Constant | 1.09049 | 0.000 |
| $\stackrel{A}{\overline{}}$ | -0.046200 | 0.000 |
| В | 0.000028 | 0.685 |
| C | -0.001118 | 0.000 |
| A^2 | 0.019601 | 0.000 |
| B^2 | -0.000009 | 0.945 |
| C^2 | 0.000001 | 0.994 |
| AB | -0.000021 | 0.782 |
| AC | 0.000879 | 0.000 |
| BC | -0.000001 | 0.987 |
| | $R^2 = 100\%$ | $R^2 - adj$ |
| Velocity | | = 100% |
| Constant | 1.16116 | 0.000 |
| A | -0.000692 | 0.000 |
| В | 0.000001 | 0.448 |
| C | -0.000017 | 0.000 |
| A^2 | 0.000315 | 0.000 |
| B^2 | 0.000000 | 0.855 |
| C^2 | 0.000000 | 0.855 |
| \overline{AB} | -0.000001 | 0.398 |
| AC | 0.000014 | 0.000 |
| BC | 0.000014 | 0.398 |
| DC | $R^2 = 100\%$ | $R^2 - adj$ |
| | h = 10070 | = 99.99% |
| Pressure | | - <i>77.7770</i> |
| Constant | -0.347475 | 0.000 |
| A | 0.001842 | 0.000 |
| В | -0.000001 | 0.729 |
| С | 0.000045 | 0.000 |
| A^2 | -0.000845 | 0.000 |
| B^2 | 0.000000 | 0.994 |
| C^2 | 0.000000 | 0.994 |
| \overline{AB} | 0.000001 | 0.805 |
| AC | -0.000038 | 0.000 |
| ВС | 0.000000 | 0.972 |
| - | $R^2 = 100\%$ | $R^2 = 100\%$ |
| | | |

$$R = 1.14775 - 0.003214A - 0.004742B$$

$$-0.067744C + 0.026980C^{2} + 0.002369AC \qquad (22)$$

$$+0.003419BC,$$

$$V = 1.00179 - 0.000049A - 0.000074B$$

$$-0.000983C + 0.000439C^{2} + 0.000041AC \qquad (23)$$

$$+0.000059BC,$$

$$P = -0.004433 + 0.000112A + 0.000166B$$

$$+0.002462C - 0.001107C^{2} - 0.000091AC \qquad (24)$$

$$-0.000133BC,$$

$$\frac{\partial R}{\partial A} = -0.003214 + 0.002369C,$$

$$\frac{\partial R}{\partial C} = -0.007744 + 0.003419C,$$

$$(25)$$

$$\frac{\partial P}{\partial C} = 0.002462 - 0.00213C,$$

$$\frac{\partial P}{\partial C} = 0.002462 - 0.002214C$$

$$-0.0000133B.$$

$$(32)$$

$$\frac{\partial R}{\partial C} = -0.067744 + 0.05396C$$

$$+0.0002369A + 0.003419B,$$

$$(27)$$

The sensitivity analysis for the radius, the velocity and the pressure when A = 0

| \boldsymbol{A} | = 0 | | | | S | ensitivity ar | nalysis | | | |
|------------------|-----|---------------------------|---------------------------|---------------------------|---------------------------|---------------------------|---------------------------|---------------------------|---------------------------|-------------------------|
| В | С | $\partial R / \partial A$ | $\partial R / \partial B$ | $\partial R / \partial C$ | $\partial V / \partial A$ | $\partial V / \partial B$ | $\partial V / \partial C$ | $\partial P / \partial A$ | $\partial P / \partial B$ | $\partial P/\partial C$ |
| | -1 | 0.001524 | 0.002096 | 0.042005 | 0.000033 | 0.000044 | 0.000804 | 0.000294 | -0.000432 | -0.002028 |
| -1 | 0 | 0.003893 | 0.005515 | 0.095965 | 0.000074 | 0.000103 | 0.001682 | 0.000385 | -0.000565 | -0.004242 |
| | 1 | 0.006262 | 0.008934 | 0.149925 | 0.000115 | 0.000162 | 0.002560 | 0.000476 | -0.000698 | -0.006456 |
| | -1 | 0.001524 | 0.002096 | 0.042518 | 0.000033 | 0.000044 | 0.000813 | 0.000294 | -0.000432 | -0.002048 |
| 0 | 0 | 0.003893 | 0.005515 | 0.096478 | 0.000074 | 0.000103 | 0.001691 | 0.000385 | -0.000565 | -0.004262 |
| | 1 | 0.006262 | 0.008934 | 0.150438 | 0.000115 | 0.000162 | 0.002569 | 0.000476 | -0.000698 | -0.006476 |
| | -1 | 0.001524 | 0.002096 | 0.043030 | 0.000033 | 0.000044 | 0.000822 | 0.000294 | -0.000432 | -0.002068 |
| 1 | 0 | 0.003893 | 0.005515 | 0.096991 | 0.000074 | 0.000103 | 0.001700 | 0.000385 | -0.000565 | -0.004282 |
| | 1 | 0.006262 | 0.008934 | 0.150951 | 0.000115 | 0.000162 | 0.002578 | 0.000476 | -0.000698 | -0.006496 |

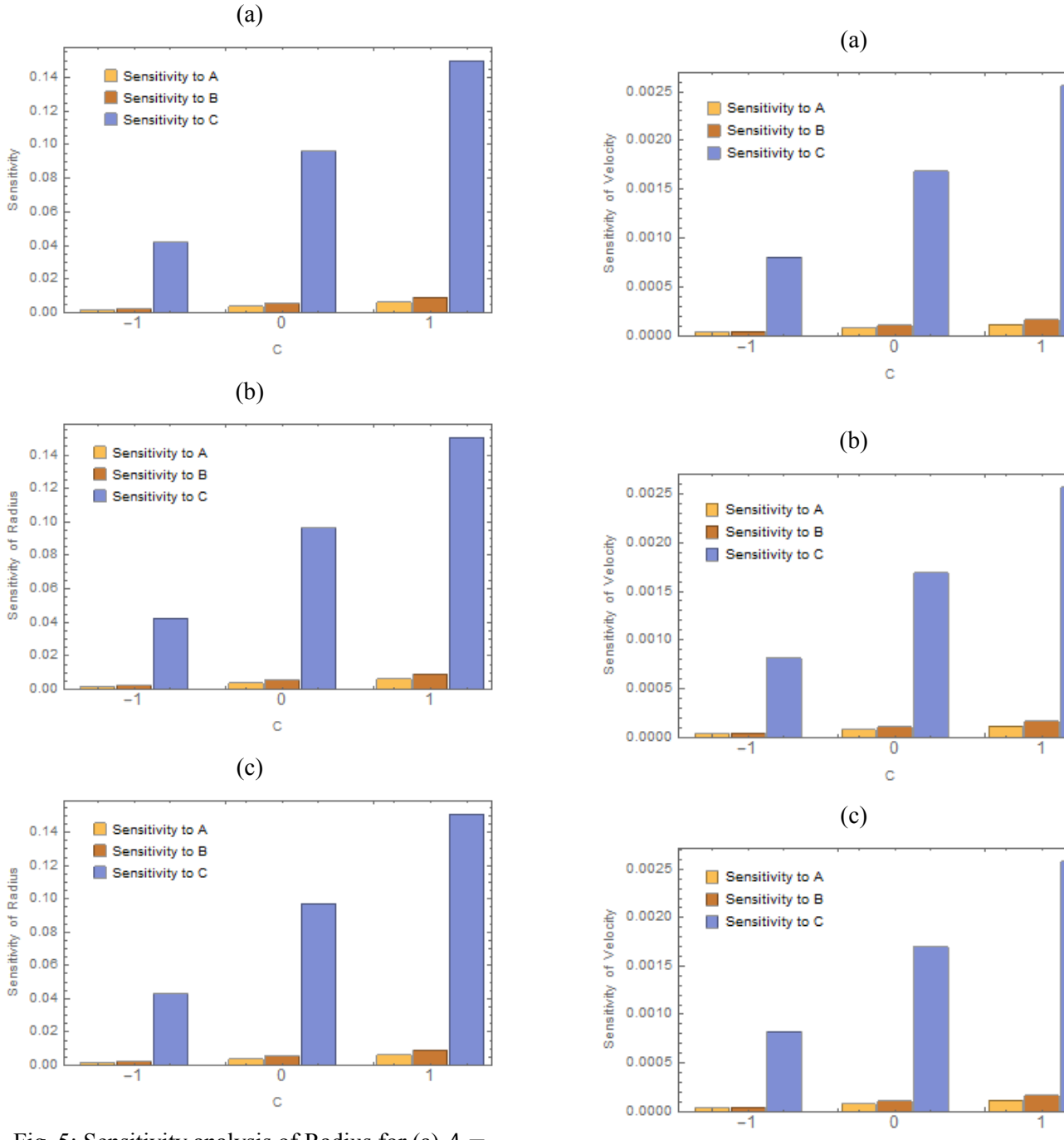
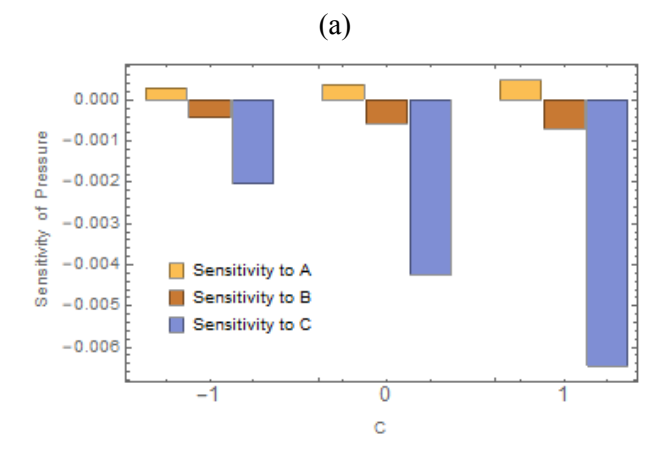
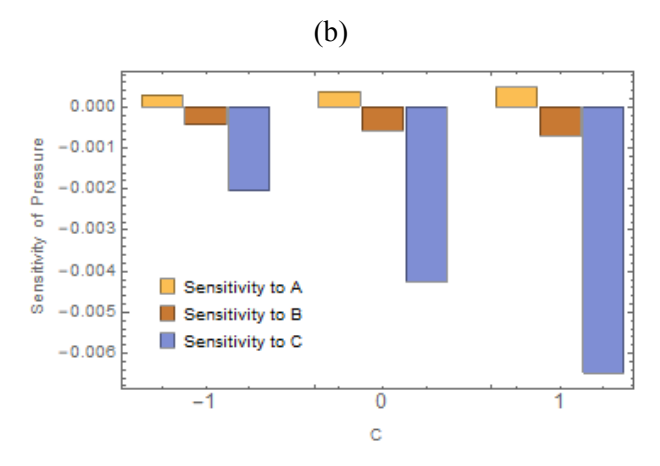


Fig. 5: Sensitivity analysis of Radius for (a) A = 0, B = -1 (b) A = 0, B = 0 (c) A = 0, B = 1

Fig. 6: Sensitivity analysis of velocity for (a) A = 0, B = -1 (b) A = 0, B = 0 (c) A = 0, B = 1

ISSN: 2367-8992 25 Volume 9, 2025





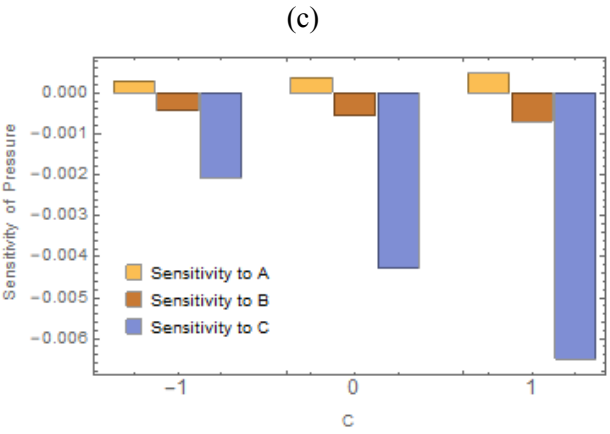


Fig. 7: Sensitivity analysis of pressure for (a) A = 0, B = -1 (b) A = 0, B = 0 (c) A = 0, B = 1

4 Results and Discussion

The graphical solution of the flow equations (15-16) and (19-21) is presented in Fig. 8-18. The parameters and their ranges used in this graphical analysis are taken as

- a. dimensionless elasticity parameter γ (0.1 to 0.3)
- b. initial void fraction α_s to be of the order $10^{-3} \text{ to } 10^{-1}$
- c. Reynolds number (100 to 1000)
- d. Number of bubbles n (1 to 3)

Fig.8 to Fig.18 helps to obtain some important observations a related to the bubbly flows in a linear elastic fluid passing through a converging-diverging Initially the bubbles (spherical) are considered to have same size and uniform distribution in the flow with each bubble having volume $V = (4/3)\pi R^3(x)$. Radius, velocity and pressure with respect to the varying parameter of elasticity are depicted in Fig. 8-10. Due to an increase in elasticity radius and velocity tends to decrease as it behaves like a damping to flow while pressure tends to increase. When more than one bubble ($n \ge 2$) are considered the same phenomena is observed. This decreasing effect is particularized in Fig. 11-13 while effects of Reynolds number are portrayed in Fig. 14-16. Increase in Reynolds number surges the radius and velocity also frequency as well as oscillations which will give escalation to cavitation in flow because of the fall of pressure.

Fig. 17 and 18 demonstrates the effects of upstream void fractions (α_s) on the radius and velocity in a flowing elastic fluid (linear elastic fluid) passing through converging-diverging nozzle. It is apparent from the graphs that the radius and velocity after passing through the throat increases while frequency oscillations decrease. In case of converging-diverging nozzle the radius and velocity increases without bound for $\alpha_s \ge 3.4 \times 10^{-2}$, which is flashing point after which flow reaches unstable region.

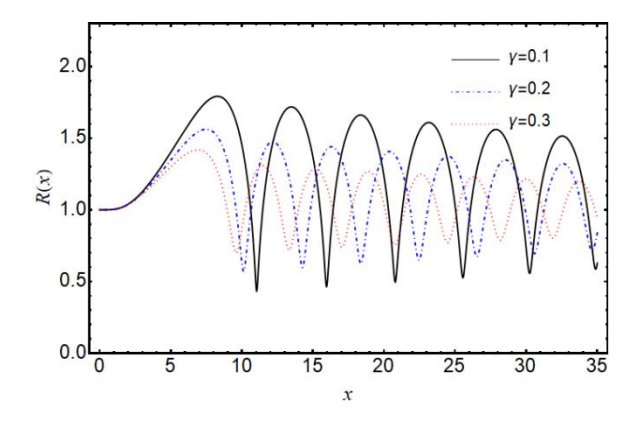


Fig. 8: Variation in radius of bubble against numerous values of elasticity parameter for flow of linear elastic fluid in a converging-diverging nozzle

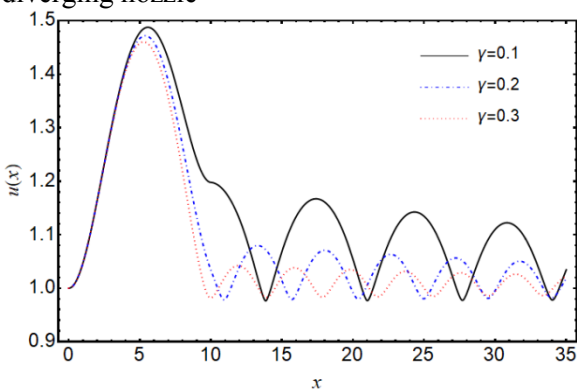


Fig. 9: Variation in radius of bubble against numerous values of elasticity parameter

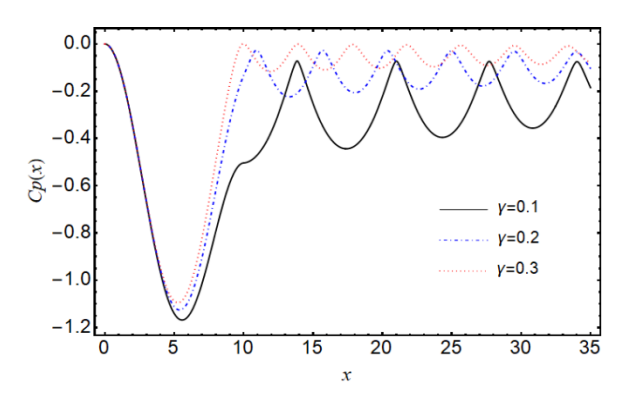


Fig. 10: Variation in pressure of bubble against numerous values of elasticity parameter for flow of linear elastic fluid in a converging-diverging nozzle

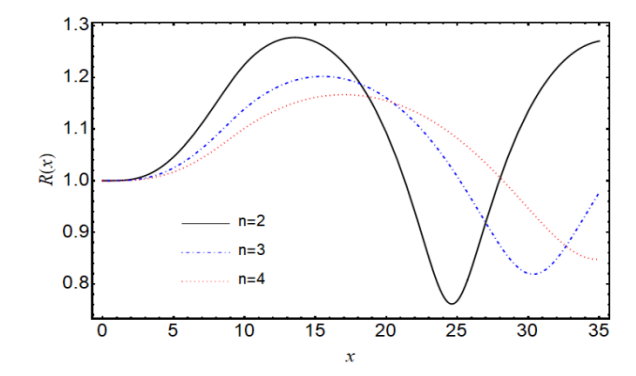


Fig. 11: Variation in radius of bubble against numerous values of number of bubbles n for flow of linear elastic fluid in a converging-

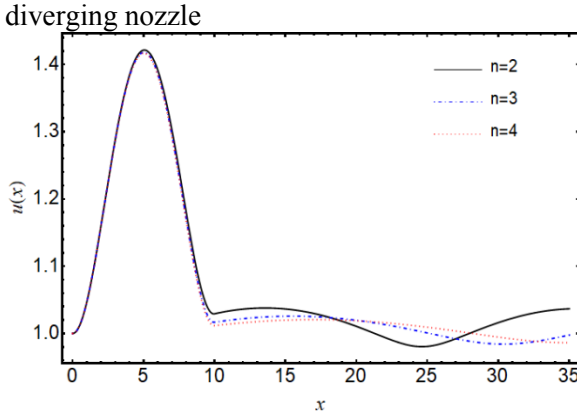


Fig. 12: Variation in velocity of the fluid for different values of the number of bubbles

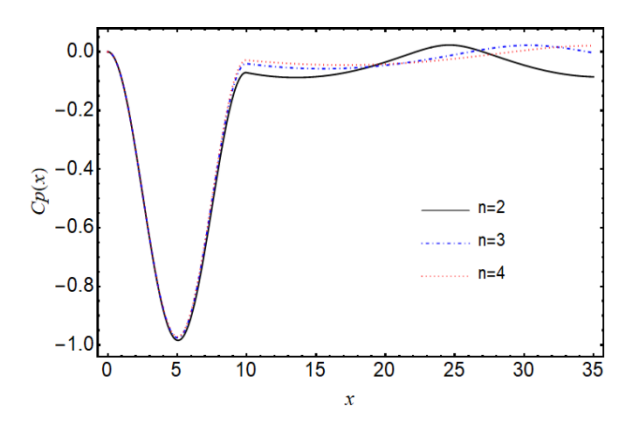


Fig. 13: Variation in pressure of the fluid for different values of the number of bubbles

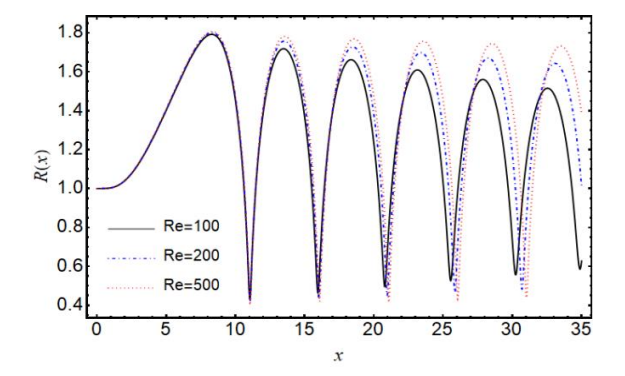


Fig. 14: Variation in radius of the bubble for different values of the Reynolds number

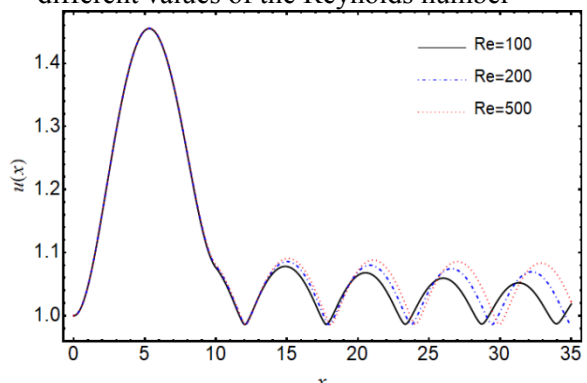


Fig. 15: Variation in velocity of the bubble for different values of the Reynolds number

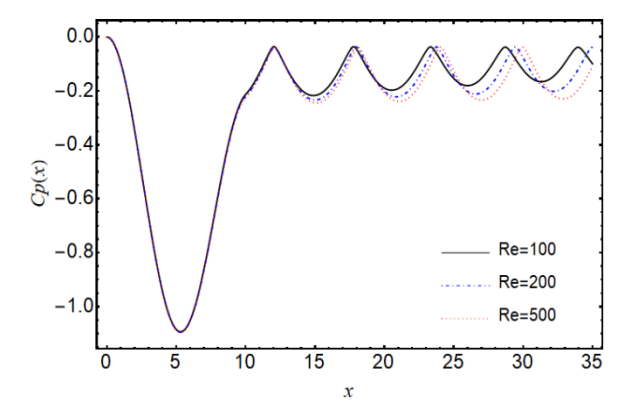


Fig. 16: Variation in pressure for different values of the Reynolds number

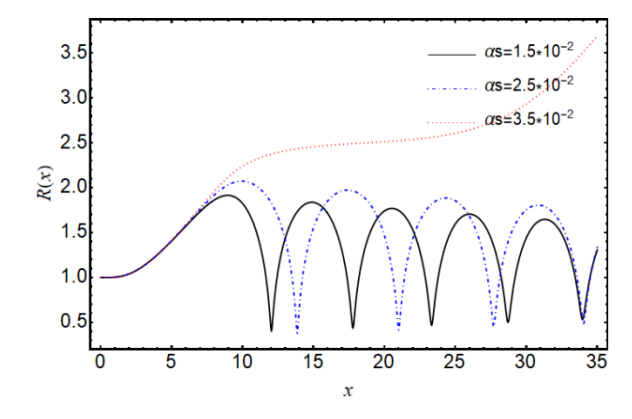


Fig. 17: Variation in radius for different values of the initial void fraction

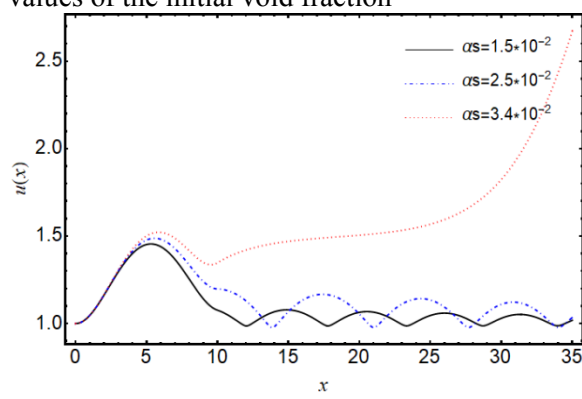


Fig. 18: Variation in velocity for different values of the initial void fraction

Discussion on the numerical results is followed by the discussion on the sensitivity of three output parameters, the radius, the velocity and pressure in response to the input parameters of the flow. The impacts of three sundry parameters, the elasticity parameter (γ), the cavitation number (σ) and the number of bubbles (n) on the three output responses the radius, velocity and the pressure coefficient are examined in this article. The optimal parameter is obtained using Response Surface Methodology (RSM) by carrying out the sensitivity analysis of the effective parameters on the flow of a cavitating unilinear elastic dimensional, fluid through converging-diverging nozzle. The ranges taken in this study of the input parameter whose responses are to be determined towards output responses are as follows:

- a. Elasticity parameter (γ) varied from 0.001 to 0.1.
- b. Cavitation number (σ) varied from 0.5 to 0.8.

ISSN: 2367-8992 28 Volume 9, 2025

c. Number of bubbles (n) varied from 1 to 4. The value of x has been set at x = 8, inside of the converging-diverging section of the nozzle to obtain the numerical data used in the analysis and presented in the **Table 2**. As per the procedure of the statistical analysis, analysis of 20 runs is performed. Numerical results for these 20 runs of the statistical analysis of all the three output variables radius, velocity and pressure obtained against the three input variables, elasticity parameter, cavitation number and number of bubbles are presented in Table 2. Using the regression coefficient the effects of performed conditions on dependent variables (radius, velocity and pressure), the variance analysis for each variable, are presented in **Tables 3** to **Table 5** respectively. From the **Tables 3** to **5** we see that due to high values of R^2 for radius, velocity and pressure, only 0.02% changes in case of radius, 0.03% changes in cases of both velocity and pressure are not admissible. Also it can be seen from the tables that all the terms are significant in analysis and are considerable whose Pvalues are above 0.05 or 5% while the terms having smaller P-values are insignificant, could be henceforth neglected. On these assumptions of the model all terms are significant except the terms A^2 , B^2 and AB as seen in Table 6 and are neglected in further analysis. Sensitivity is plotted in Figs. 5-7 using bar diagrams for better understanding. Figs. 5 (a-c) is plotted for A = 0, in Fig. 5 (a) B = -1 that is $\gamma = 0.5$, in Fig. 5 (b) B = 0 that is $\gamma = 0.0505$ while in Fig. 5 (c) B = 1 that is $\gamma = 0.1$ is considered. In all figs. 5(a-c) C assumes the values -1, 0 and 1. In the stated conditions, the sensitivity of radius shown in Figs. 5 (a-c) increases with the increase in value C. Same is the case for sensitivity of velocity in Figs. 6 (a-c) while in case of pressure increasing values of C. results in the decrease in sensitivity of pressure.

5 Conclusion

The study carried out to investigate the influence of emerging parameters on the flow behavior of bubbly-cavitating flow of linear elastic fluid flowing across the nozzle (converging-diverging nozzle) described in **Fig. 1**. Apart from the fact that two flow regimes are possible, we have only discussed the flow behavior in stable region despite of finding the critical point for bifurcation to occur. Large-scale spatial fluctuations are noted, even a small value of void fraction creates fluctuations in the flow, other

parameters also effects significantly. An increase in velocity and decrease in pressure is clearly consequence of the Bernoulli's principle. To observe the effects of the elasticity parameter, the cavitation number and the number of bubbles in the flow we have studied sensitivity of the parameters towards unknown variables radius, velocity and pressure. According to earlier research on cavitation in viscoelastic media, overall elasticity acts to lessen the abrasiveness of collapse and development compared to the behavior in a Newtonian medium. Depending on the constitutive model, the elastic terms have varying coefficients and exponents that are dependent on the deviation from the initial configuration. As one might anticipate, these phrases stand for an elastic restoring force, or a spring. The constitutive model may have a substantial impact on the bubble response. Here likewise we see that increasing in values of C that is the number of bubbles in flow is most prominent among the other parameters. Increase in value of C cause an increase in sensitivity of the radius as well as velocity while increase in value of C causes a decrease in sensitivity of pressure as the case may be due to satisfaction of Bernoulli's principle. In all the cases sensitivity of radius and velocity to A (elasticity), B (cavitation number) and C (the number of bubbles) increases while pressure decreases in irrespective of the fact in first case it is positive while in other cases it is negative. It is important to note that this sensitivity analysis has been carried out in the converging diverging section of the nozzle for some specific value of horizontal axis. We cannot generalize it for the whole domain anyhow we could examine the behavior where needed. When we look at the Figs. 5-7, we observe that there is not a significant change from fig. a-c, it means by changing input values this behavior is unaltered.

6 Nomenclature

| We | Weber Number |
|------------------|---|
| \boldsymbol{A} | Nozzles' cross-section area m^2 |
| и | Velocity of flow |
| η | Bubble Population |
| α | The void fraction of the bubbly mixture |
| $ ho_l$ | Density of the fluid |

 \mathbf{D}

| R | Radius of bubble |
|----------|---------------------------------------|
| t | Time |
| Cp | Fluid pressure coefficient |
| P | Fluid pressure |
| L | Length of the nozzle |
| μ | Dynamic viscosity of the fluid |
| S | Surface tension |
| σ | Cavitation number |
| β | Second-Grade fluid parameter |
| Re | Reynolds number |
| P_G | Non-condensable gas inside the bubble |
| х | Eulerian coordinates |

Dading of bubble

References:

- [1] C. E. Brennen, Cavitation and bubble dynamics. Cambridge university press (2014)
- [2] T. Leighton, The acoustic bubble. Academic press (2012)
- [3] D. Wittekind, M. Schuster, Propeller cavitation noise and background noise in the sea. Ocean Engineering 120 (2016) 116-121, https://doi.org/10.1016/j.oceaneng.2015.12.060
- [4] R. B. Bird, R. C. Armstrong, & O. Hassager, Dynamics of polymeric liquids: Fluid mechanics Vol. 1 (1987)
- [5] Shima, A., Rajvanshi, S. C., & Tsujino, T. Study of nonlinear oscillations of bubbles in Powell–Eyring fluids. The Journal of the Acoustical Society of America 77(5) (1985) 1702-1709, https://doi.org/10.1121/1.391917
- [6] T. Tsujino, A. Shima, Y. Oikawa, J. Sound Vib., 123, 171 (1988).
- [7] E. A. Brujan, The effect of polymer concentration on the non-linear oscillation of a bubble in a sound-irradiated liquid. Journal of sound and vibration 173(3) (1994) 329-342, https://doi.org/10.1006/jsvi.1994.1234
- [8] A. Shima, T. Tsujino, H. Nanjo, Nonlinear oscillations of gas bubbles in viscoelastic fluids. Ultrasonics, 24(3) (1986) 142-147, https://doi.org/10.1016/0041-624X(86)90054-5
- [9] R. Y. Ting, Effect of polymer viscoelasticity on the initial growth of a vapor bubble from gas nuclei. The Physics of Fluids 20(9) (1977) 1427-1431, https://doi.org/10.1063/1.862038
- [10] L. Fang, X. Xu, A. Li, Z. Wang, Q. Li. Numerical investigation on the flow characteristics and choking mechanism of cavitation-induced choked flow in a Venturi

- reactor. Chem. Eng. J. 423 (2021) 130234, https://doi.org/10.1016/j.cej.2021.130234
- [11] Fogler, H. S., & Goddard, J. D. Collapse of spherical cavities in viscoelastic fluids. The Physics of Fluids, 13(5) (1970) 1135-1141, https://doi.org/10.1063/1.1693042
- [12] Fogler, H. S., & Goddard, J. D. Oscillations of a gas bubble in viscoelastic liquids subject to acoustic and impulsive pressure variations. J. of Appl. Phy., 42(1) (1971) 259-263, https://doi.org/10.1063/1.1659578
- [13] A. Shima, T. Tsujino, The behaviour of bubbles in polymer solutions. Chem. Eng. Sc., 31(10) (1976) 863-869, https://doi.org/10.1016/0009-2509(76)87035-2
- [14] J.S. Allen, R. A. Roy, Dynamics of gas bubbles in viscoelastic fluids. I. Linear viscoelasticity, J. Acoust. Soc. Am., 107(6) (2000) 3167-3178, https://doi.org/10.1121/1.429344
- [13] Allen, J. S., & Roy, R. A. Dynamics of gas bubbles in viscoelastic fluids. II. Nonlinear viscoelasticity, J. Acoust. Soc. Am., 108(4) (2000)1640-1650, https://doi.org/10.1121/1.1289361
- [15] R. Gaudron, M. T. Warnez, E. Johnsen, Bubble dynamics in a viscoelastic medium with nonlinear elasticity, J. Fluid Mech., 766 (2015) 54-75, https://doi.org/10.1017/jfm.2015.7
- [16] R. F. Tangren, C. H. Dodge, H. S. Seifert, Compressibility effects in two-phase flow, J. Appl. Phys., 20(7) (1949) 637-645, https://doi.org/10.1063/1.1698449
- [17] Y. C. Wang, C. E. Brennen, One-dimensional bubbly cavitating flows through a converging-diverging nozzle, J. Fluids Eng. (1998) 166-170, https://doi.org/10.1115/1.2819642
- [18] A. H. Thaker, K. R. Madane, V. V. Ranade, Influence of viscosity and device scale on pressure drop and cavitation inception: Vortex based cavitation devices, Chem. Eng. J., (2023) 145943, https://doi.org/10.1016/j.cej.2023.145943
- [19] Z. A. Mohammed, K. E. Mohand, Analysis of cavitating flow through a venturi, Sci. Res. Essays, 10(11) (2015) 367-375, https://doi: 10.5897/SRE2015.6201
- [20] M. S. Nadeem, A. Zeeshan, F. Alzahrani, Numerical simulation of unidimensional bubbly flow in linear and non-linear one parameter elastic liquid through a nozzles, Eur. Phys. J.: Spec. Top., 231(3) (2022) 571-581, https://doi.org/10.1140/epjs/s11734-022-00441-9
- [21] A. Zeeshan, M. S. Nadeem, F. Alzahrani, Numerical simulation of unidimensional bubbly flow in Mooney Rivlin fluid through nozzles and a wavy channel, Waves Random Complex Media, (2022) 1-15, https://doi.org/10.1080/17455030.2022.2117876
- [22] J. Hao, M. Zhang, X. Huang, Experimental study on influences of surface materials on cavitation flow around hydrofoils, Ch. J. Mech. Eng. EN, 32 (2019) 1-11, https://doi.org/10.1186/s10033-019-0355-5

- [23] A. Prosperetti, L. A. Crum, K. W. Commander, Nonlinear bubble dynamics, J. Acoust. Soc. Am., 83(2) (1988) 502-514, https://doi.org/10.1121/1.396145
- [24] M. Imtiaz, F. Mabood, T. Hayat, A. Alsaedi, Homogeneous-heterogeneous reactions in MHD radiative flow of second grade fluid due to a curved stretching surface, Int. J. Heat Mass Transf., 145 (2019) 118781, https://doi.org/10.1016/j.ijheatmasstransfer.2019.118781
- [25] M. S. Plesset, A. Prosperetti, Bubble dynamics and cavitation, Ann. Rev. fluid mech., 9(1) (1977) 145-185, https://doi.org/10.1146/annurev.fl.09.010177.001045
- [26] T. Hayat, S. Nadeem, S. Asghar, Periodic unidirectional flows of a viscoelastic fluid with the fractional Maxwell model, Appl. Math. Comput., 151(1) (2004) 153-161, https://doi.org/10.1016/S0096-3003(03)00329-1
- [27] T. Hayat, M. Sajid, I. Pop, Three-dimensional flow over a stretching surface in a viscoelastic fluid, Nonlinear Anal. Real World Appl., 9(4) (2008) 1811-1822, https://doi.org/10.1016/j.nonrwa.2007.05.010
- [28] M. M. Bhatti, M. Marin, A. Zeeshan, R. Ellahi, S. I. Abdelsalam, Swimming of motile gyrotactic microorganisms and nanoparticles in blood flow through anisotropically tapered arteries, Front. Phys., 8 (2020) 95, https://doi.org/10.3389/fphy.2020.00095
- [29] L. Codarcea-Munteanu, M. Marin, Micropolar thermoelasticity with voids using fractional order strain. Models and Theories in Social Systems, (2019) 133-147, https://doi.org/10.1007/978-3-030-00084-4_7
- [30] K. R. Rajagopal, A. S. Gupta, A. S. On a class of exact solutions to the equations of motion of a second grade fluid. Int. J. Eng. Sci., 19(7) (1981) 1009-1014, https://doi.org/10.1016/0020-7225(81)90135-X
- [31] R. L. Fosdick, K. R. Rajagopal, Uniqueness and drag for fluids of second grade in steady motion, Int. J. Non Linear Mech., 13(3) (1978) 131-137, https://doi.org/10.1016/0020-7462(78)90001-X
- [32] D. Dubin, S. Diego, Numerical and analytical methods for scientists and engineers using Mathematica (Vol. 1). Hoboken, NJ. Wiley-Interscience. (2003)
- [33] K. M. Shirvan, R. Ellahi, S. Mirzakhanlari, M. Mamourian, Enhancement of heat transfer and heat exchanger effectiveness in a double pipe heat exchanger filled with porous media: Numerical simulation and sensitivity analysis of turbulent fluid flow, Appl. Therm. Eng.,109 (2016) 761-774, https://doi.org/10.1016/j.applthermaleng.2016.08.116
- [34] S. Q. Chan, F. Aman, S. Mansur, Sensitivity analysis on thermal conductivity characteristics of a water-based bionanofluid flow past a wedge surface, Math. Probl. Eng., (2018) 1-12, https://doi.org/10.1155/2018/9410167
- [35] D. Hussain, Z. Asghar, A. Zeeshan, H. Alsulami, Analysis of sensitivity of thermal conductivity and variable viscosity on wall heat flux in flow of viscous fluid

over a porous wedge, Int. Commun. Heat Mass Transf., , 135 (2022) 106104, https://doi.org/10.1016/j.icheatmasstransfer.2022.106104

ISSN: 2367-8992 31 Volume 9, 2025